Characterization of gold supported on Al$_2$O$_3$–CuO–Mn$_2$O$_3$ catalysts obtained by thermal decomposition of aerosols

Barbara Małecka · Maria Rajska

Abstract Gold ($\sim$1%) has been supported on the mixed oxides Al$_2$O$_3$–CuO–Mn$_2$O$_3$ with molar compositions 1:1:1, 1:0.7:0.3, 1:0.3:0.7, prepared by spray pyrolysis method. The supports and catalysts have been characterized by TG, DTA, N$_2$ physisorption, XRD, SEM, and TEM methods and tested for CO oxidation (25–300 °C). The catalysts revealed high specific surface area and amorphous form for compositions 1:0.7:0.3 and 1:0.3:0.7. Gold deposited on the supports lowered the T_{50} values by 50–80 °C. The highest CO conversion was obtained for 1:1:1 composition.

Keywords TG · DTA · Spray pyrolysis · Gold catalysts · Transition metal oxides · Oxidation of CO

Introduction

Twenty years ago Haruta and coworkers discovered that gold is active for heterogeneous oxidative reactions at low temperatures [1]. This was the inspiration for many investigations of this new, interesting behavior of gold which showed, that CO oxidation [2, 3], selective oxidation of alkanes [4], reduction of NO$_x$ [5], glucose oxidation [6], synthesis of hydrogen peroxide [7], and a lot more reactions are catalyzed by gold [8, 9].

Gold exhibits a unique catalytic nature and action when it is deposited as nanoparticles on a metal oxide. The typical supported gold catalyst consists of gold nanoparticles of various sizes and shapes dispersed on an amorphous support, usually a high-area metal oxide powder. Support seems to play different role. First, support keeps nanocrystallites of gold apart and stabilizes them against sintering [10], which could produce larger crystallites and in consequence reduce catalytic properties. Second, it is well established that the catalytic reaction proceeds at the edges of gold particles involving either gold atoms influenced by the support or sites on the adjacent support [11].

A large number of metal oxide supports have been reported in the literature. Gold catalysts on a single oxide support were extensively studied, among them Al$_2$O$_3$ [12, 13] and many oxides of the transition metals. Al$_2$O$_3$ is a most common kind of oxide used as support in industrial catalytic process. Al$_2$O$_3$ is regarded as an inert support material for gold catalysts and its role lies in high specific surface area. Catalysts consisting of gold supported on reducible oxides like TiO$_2$, Fe$_3$O$_4$, Co$_3$O$_4$, MnO$_2$ are more active toward CO and propene oxidation or NO$_x$ reduction than those supported on nonreducible oxides [14–17]. This probably results from synergistic effects between the gold nanoparticles and support material and the varying ability of the supports to supply oxygen to facilitate the oxidation reaction [18, 19]. One of the proposed pathways of the reaction assumes that CO oxidation occurs at the metal/support interface on Au–O vacancy sites and requiring O atoms are provided by the support.

Although studies on gold-supported catalysts have been widely reported in the literature, the use of mixed oxides to combine the chemical properties of reducible oxides with the physical properties of traditional oxides, such as Al$_2$O$_3$, has been little studied. The investigations on gold catalysts supported on different mixed oxides MO$_x$/Al$_2$O$_3$ with M = Ce, Fe, Co, Mn [16, 20–22] and M^{I}O$_x$/M^{II}O$_x$/Al$_2$O$_3$ with M^I, M^{II} = Li, Rb, Mg, Co, Mn, Ce, La, Ti [23, 24] were reported. For CO oxidation on multicomponent gold

B. Małecka (✉) · M. Rajska
Faculty of Materials Science and Ceramics, AGH University
of Science and Technology, 30. Mickiewicz Av.,
30-059 Krakow, Poland
e-mail: bmalecka@agh.edu.pl

catalysts it has been suggested that oxides of transition metals play an important role in O_2 activation via a Mars and Van Krevelen-type mechanism.

In this study gold supported on $Al_2O_3/CuO/Mn_2O_3$ catalysts were studied. The support was prepared in the one-step process by spray pyrolysis of the solution of salts mixture and gold was deposited by deposition–precipitation procedure. This is well-tried method of introducing gold to the catalyst. The possibility of obtaining nanocrystalline gold by thermal decomposition of its salt is reported in [25] but not verified.

Manganese oxides (MnO_x) have long been used as highly active, durable, and low cost catalysts for the combustion of various volatile organic substances or hydrocarbons [26, 27]. Together with gold nanoparticles the significantly improved activity has been achieved over Au/MnO_x system for low-temperature CO oxidation [28, 29]. The manganese oxide added to Fe_2O_3/Al_2O_3 gave the progressive increase of the catalytic activity of this system [30].

Copper oxides have a large variety of potential applications with regard to unique tunable physical properties. Copper oxide is applied as heterogeneous catalyst in environmental processes [31, 32], in water–gas shift reaction [33], in solid-state gas sensors [34, 35], and oxidation of aromatic hydrocarbons [36]. The addition of copper oxide to cerium oxide resulted in increased activity of $CuO–CeO_2$ catalyst toward CO oxidation [37, 38].

The goal of this study was to produce, characterize, and test the catalytic activity for CO oxidation of the gold supported on the mixed transition metal oxides and alumina $Al_2O_3–CuO–Mn_2O_3$ catalysts.

Experimental

Catalyst preparation

The supports of mixed metal oxides were synthesized by spray pyrolysis method [39, 40]. The starting materials used were $Al(NO_3)_3 \cdot 9H_2O$, $Cu(NO_3)_2 \cdot 3H_2O$, and $Mn(NO_3)_2 \cdot 4H_2O$ (POCH S.A.). The aqueous solutions of mixture of metal nitrates with appropriate ratios were prepared. The concentration of metal nitrates solutions was 0.12 mol dm^{-3}. The spray pyrolysis system consisted of an ultrasonic nebulizer, a quartz tube reactor, furnace, and an electrostatic filter. The obtained solutions were atomized by the ultrasonic nebulizer (frequency: 2.6 MHz) and then transported by a carrier gas (air, flow rate 100 $\text{cm}^3 \text{ min}^{-1}$) into the quartz reactor placed in the furnace where pyrolysis occurred at 700 °C. For collecting of the obtained oxide powders an electrostatic filter at the outlet of the reactor was used. In result the mixed oxides with three

different molar compositions were obtained: $Al_2O_3–CuO–Mn_2O_3$ (1:1:1), $Al_2O_3–0.3CuO–0.7Mn_2O_3$ (1:0.3:0.7), and $Al_2O_3–0.7CuO–0.3Mn_2O_3$ (1:0.7:0.3).

The gold catalysts were prepared by deposition–precipitation method with the solution of $HAuCl_4$ of concentration $0.00175 \text{ mol dm}^{-3}$ as a precursor of the active gold phase. The gold solution was heated to 70 °C and, while stirring, the support was added. The pH of the suspension was kept at 7 with diluted NaOH. The suspension was cooled down and solids were separated from the solution by centrifugation and washed with distilled water in order to remove the chloride and Na^+ ions. Next, samples were dried overnight at 40 °C in air. Calcination of the samples was performed at 300 °C for 2 h in air prior before catalytic activity tests. The theoretical loading of Au was 1 wt% in all the samples.

Characterization methods

The X-ray powder diffraction (XRD) patterns were obtained in a Philips model PW 3710 diffractometer equipped with adapter for low-angular geometry GID using Cu K_α radiation ($\lambda = 0.15418$ nm).

The specific surface area of the samples was determined by BET method using nitrogen adsorption–desorption isotherms with ASAP 2010 Micromeritics.

Transmission electron microscope (TEM) images were acquired with a JEOL-JEM1011 (100 kV; magnification 500,000). Diluted suspensions of samples in ethanol were prepared and drop-dried on carbon-coated copper TEM grids. TEM images were used for determination of the distribution of particle diameter on the basis of 200 particles.

The morphological characteristics of the particles were investigated using JEOL 5400 scanning electron microscope (SEM).

Thermogravimetry analysis (TG) and differential thermal analysis (DTA) were carried out on a thermal analyzer SDT 2960 TA Instruments in synthetic air (21% O_2, 79% N_2), the rate of temperature increase $\beta = 5$ °C min^{-1}. The mixtures of nitrates for thermal analysis experiments were prepared by dissolving of appropriate amounts of metal nitrates in water and drying the obtained solution at room temperature on air.

Catalytic activity measurements

The catalytic activity tests were performed at atmospheric pressure in fixed-bed quartz flow reactor (i.d. 10 mm). The catalyst weight was 300 mg, and the total flow rate of the reaction gas was 100 $\text{cm}^3 \text{ min}^{-1}$, with a composition of 1, 2, and 3% CO balanced with synthetic air (gas hourly space velocity 500, 1000, 1500 h^{-1}, respectively, calculated for

CO). The catalyst samples were diluted with chemically inert glass balls.

Prior to measurements the catalysts were heated at 300 °C in air for 30 min in order to standardize the sample. Next the reactor was cooled down under a flow of air before introducing the reactant flow. In every catalytic test, the reaction temperature was stepwisely increased from 25 up to 300 °C.

The composition of the effluent gas was detected online by quadrupole mass spectrometer ThermoStar GSD 300^T Balzers Instruments. The conversion of CO was calculated based on the formation of CO$_2$ and its concentration in the effluent gases using calibration curve measured for different compositions of the inlet gas.

Results and discussion

Thermal analysis

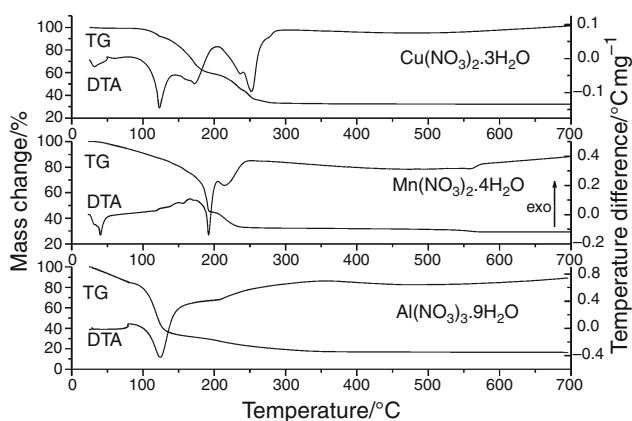Figures 1 and 2 show the TG–DTA curves obtained during decomposition of individual aluminum, copper, and

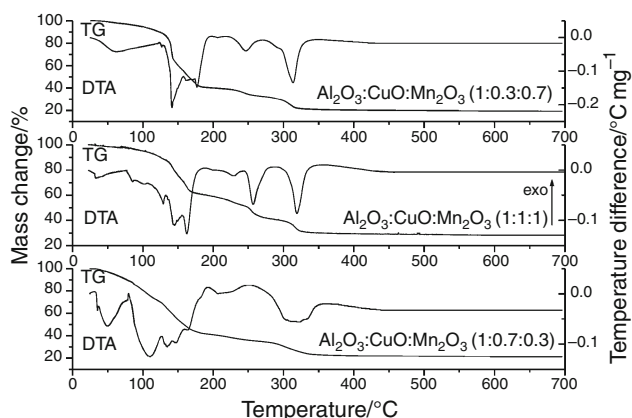**Fig. 1** TG–DTA results of decomposition of metal nitrates (air, 5 °C min^{-1})

Fig. 2 TG–DTA results of decomposition of mixtures of metal nitrates (air, 5 °C min^{-1})

manganese nitrates and mixtures of these three metal nitrates with compositions used in this study, respectively. As can be seen from Fig. 1 the temperatures of the end of decomposition of individual metal nitrates are: 250 °C for Mn(NO$_3$)$_2$·4H$_2$O, 280 °C for Cu(NO$_3$)$_2$·3H$_2$O, and 340 °C for Al(NO$_3$)$_3$·9H$_2$O. At these temperatures MnO$_2$, CuO, and AlOOH form. When temperature raised to 600 °C, MnO$_2$ decomposed further to Mn$_2$O$_3$ and AlOOH to γ-Al$_2$O$_3$ [41–43]. The decomposition of mixtures of three nitrates is not a simple superposition of the curves obtained for each individual metal nitrate. Comparing DTA curves from Figs. 1 and 2 one can see that new peak with minimum at 315 °C appeared for decomposition of nitrates mixtures. This effect can be connected with new compounds which have formed in result of the procedure of mixing. Most probably the co-precipitation of mixed salts like MnCu(NO$_3$)$_4$ or MnAl(NO$_3$)$_5$ or AlCu(NO$_3$)$_5$ has occured. All the nitrates mixtures were completely decomposed at 400 °C; thus, the temperature 700 °C chosen for the preparation of the samples by spray pyrolysis method guaranteed that mixed oxides can be obtained.

Characterization of the catalysts and supports

All measurements were made both on the supports and on the finished catalysts. BET specific surface areas of the samples are given in Table 1. The results show that the treatment of the samples connected with gold deposition gave the significant increase in the specific surface area of all the samples.

Figures 3, 4, and 5 show the X-ray diffraction patterns of bare supports and Au-loaded supports. All XRD patterns display the highly amorphous form of the samples especially of the bare supports. This is consistent with the specific surface areas obtained. XRD reflections characteristic of Mn$_2$CuO$_4$ (JCPDS–ICDD PDF2 (01-076-2296)) and Al$_2$CuO$_4$ (JCPDS–ICDD PDF2 (01-076-2295)) phases were present in the patterns of bare supports of composition Al$_2$O$_3$–CuO–Mn$_2$O$_3$: (1:1:1) and (1:0.7:0.3). In the case of (1:0.3:0.7) specimen only one weak Mn$_2$CuO$_4$ reflection was present. No diffraction lines corresponding to simple metal oxides were found. In the XRD patterns of the Au-loaded samples for (1:0.7:0.3) and (1:0.3:0.7) compositions only one–two very weak signals of triple

Table 1 Characterization of the catalysts and supports

Sample	S$_{BET}$/m^2 g^{-1}		T$_{50}$/°C	
	Support	1% Au	Support	1% Au
Al$_2$O$_3$–CuO–Mn$_2$O$_3$ (1:1:1)	141	175	226	142
Al$_2$O$_3$–CuO–Mn$_2$O$_3$ (1:0.3:0.7)	181	229	233	188
Al$_2$O$_3$–CuO–Mn$_2$O$_3$ (1:0.7:0.3)	107	189	246	178
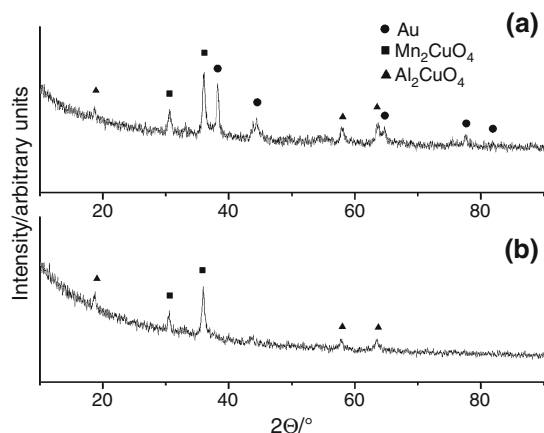
Fig. 3 XRD pattern of: **a** 1% Au/Al$_2$O$_3$–CuO–Mn$_2$O$_3$ (1:1:1), **b** Al$_2$O$_3$–CuO–Mn$_2$O$_3$ (1:1:1)
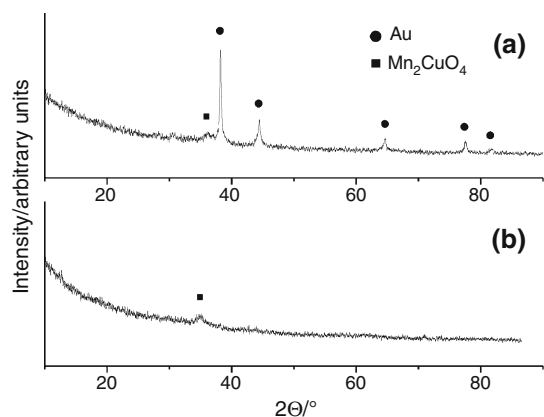
Fig. 4 XRD pattern of: **a** 1% Au/Al$_2$O$_3$–CuO–Mn$_2$O$_3$ (1:0.3:0.7), **b** Al$_2$O$_3$–CuO–Mn$_2$O$_3$ (1:0.3:0.7)
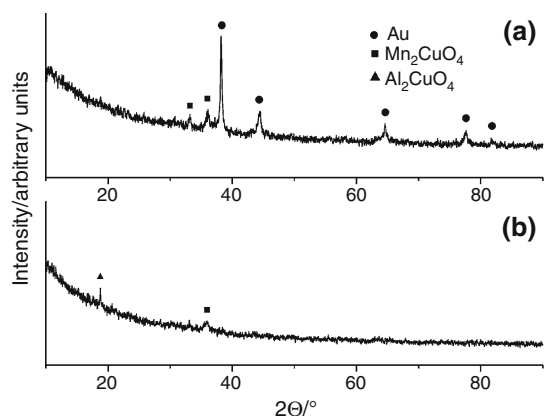
Fig. 5 XRD pattern of: **a** 1% Au/Al$_2$O$_3$–CuO–Mn$_2$O$_3$ (1:0.7:0.3), **b** Al$_2$O$_3$–CuO–Mn$_2$O$_3$ (1:0.7:0.3)

oxide phases were detected, which shows that samples have amorphous form. The reflections of Au were additionally observed.

SEM images (Figs. 6a, 7a, 8a) of the supports show the ball-shape form of the grains of all the samples. This shape
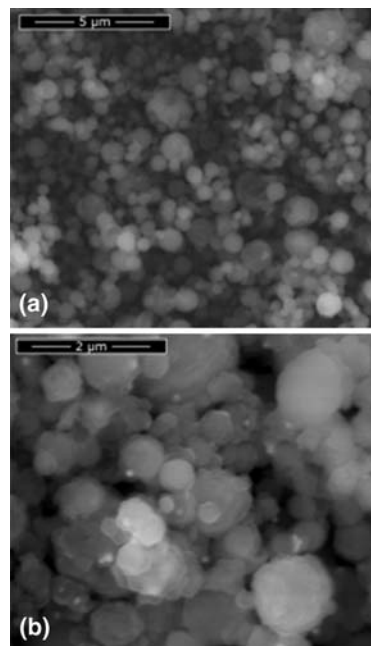

Fig. 6 SEM images of: **a** Al$_2$O$_3$–CuO–Mn$_2$O$_3$ (1:1:1), **b** 1% Au/Al$_2$O$_3$–CuO–Mn$_2$O$_3$ (1:1:1)
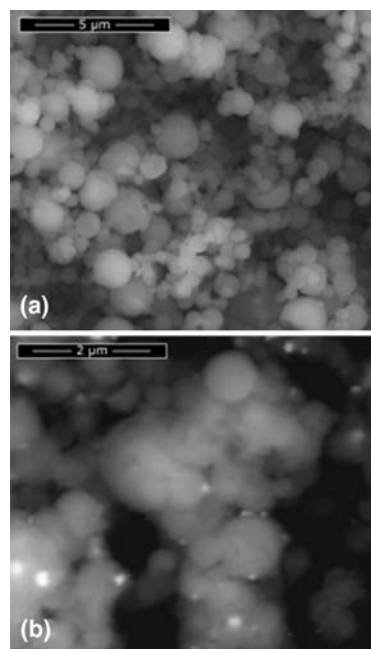
Fig. 7 SEM images of: **a** Al$_2$O$_3$–CuO–Mn$_2$O$_3$ (1:0.3:0.7), **b** 1% Au/Al$_2$O$_3$–CuO–Mn$_2$O$_3$ (1:0.3:0.7)

did not change after the procedure of the deposition of gold (Figs. 6b, 7b, 8b). TEM image (Fig. 9) clearly shows that Au particles are randomly distributed within the support grain. The size distribution of gold particles calculated on the basis of TEM images revealed that most of the gold particles have diameter in the range 6–18 nm (Fig. 10).
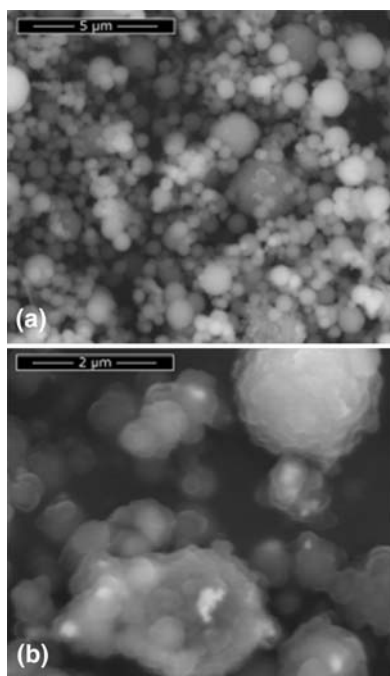
Fig. 8 SEM images of: **a** Al$_2$O$_3$–CuO–Mn$_2$O$_3$ (1:0.7:0.3), **b** 1% Au/Al$_2$O$_3$–CuO–Mn$_2$O$_3$ (1:0.7:0.3)
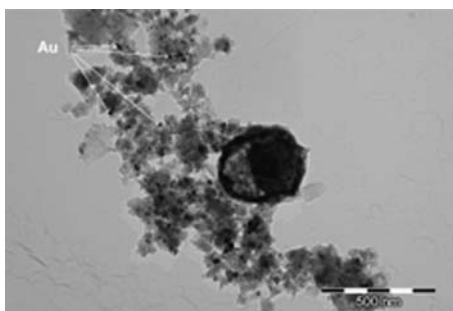

Fig. 9 TEM image 1% Au/Al$_2$O$_3$–CuO–Mn$_2$O$_3$ (1:1:1)

Activity for CO oxidation

The activity tests were performed up to 300 °C because higher temperatures could lead to the segregation of gold resulting in lowering catalytic activity. The temperature-conversion plots for the supports and catalysts are shown in Fig. 11 for 1% CO in reaction gas as example (the conversions in respect of temperature for other CO contents were the same). None of the sample showed 100% activity. All the supports revealed similar activity toward CO oxidation. It should be pointed out that for all samples oxidation of CO started at about 50 °C. Gold deposited on the supports lowered the temperature of 50% conversion, T_{50}, by 50–80 °C (Table 1). The best results of catalysts activity toward the oxidation of CO were obtained for the sample Au/Al$_2$O$_3$–CuO–Mn$_2$O$_3$ (1:1:1).
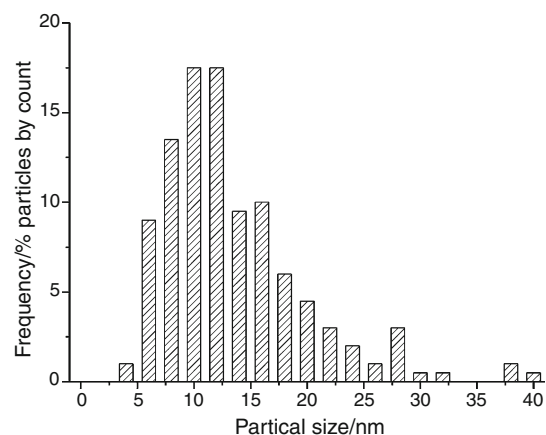

Fig. 10 Distribution of Au particle size for 1% Au/Al$_2$O$_3$–CuO–Mn$_2$O$_3$ (1:1:1) calculated for 200 Au particles
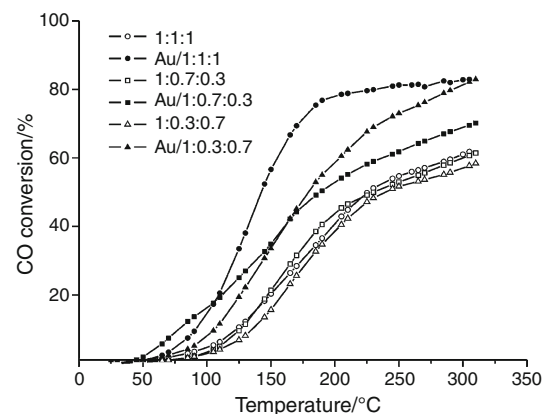

Fig. 11 Activity toward CO oxidation of supports and 1% Au-loaded Al$_2$O$_3$–CuO–Mn$_2$O$_3$ of different compositions (1% CO in reactant gas)

Summary

The spray pyrolysis method was successfully applied for obtaining Al$_2$O$_3$–CuO–Mn$_2$O$_3$ supports of different compositions. The obtained materials have very high specific surface area and amorphous form. The deposition of gold (1%) significantly increased the specific surface area, particularly for sample with (1:0.7:0.3) composition. The most of gold particles have diameter in the range 6–18 nm. Gold deposited on the supports lowered the values of T_{50} by 50–80 °C. The best activity toward CO oxidation was obtained for the sample Au/Al$_2$O$_3$–CuO–Mn$_2$O$_3$ (1:1:1).

References

1. Haruta M, Yamada N, Kobayashi T, Iijima S. Gold catalysts prepared by coprecipitation for low-temperature oxidation of hydrogen and of carbon monoxide. J Catal. 1989;115:301–9.

2. Tseng Ch-H, Yang TCK, Wu H-E, Chiang H-Ch. Catalysis of oxidation of carbon monoxide on supported gold nanoparticle. J Hazard Mater. 2009;166:686–94.

3. Min BK, Friend CM. Heterogeneous gold-based catalysis for green chemistry: low-temperature CO oxidation and propene oxidation. Chem Rev. 2007;107:2709–24.

4. Hughes MD, Xu Y-J, Jenkins P, McMorn P, Landon P, Enache DI, et al. Tunable gold catalysts for selective hydrocarbon oxidation under mild conditions. Nature. 2005;437:1132–5.

5. Nguyen LQ, Salim Ch, Hinode H. Performance of nano-sized Au/TiO$_2$ for selective catalytic reduction of NOx by propene. Appl Catal A. 2008;347:94–9.

6. Baatz C, Decker N, Prüße U. New innovative gold catalysts prepared by an improved incipient wetness method. J Catal. 2008;258:165–9.

7. Landon P, Collier PJ, Carley AF, Chadwick D, Papworth AJ, Burrows A, et al. Direct synthesis of hydrogen peroxide from H$_2$ and O$_2$ using Pd and Au catalysts. Phys Chem Chem Phys. 2003;5:1917–23.

8. Cárdenas-Lizana F, Gómez-Quero S, Keane MA. Gas phase hydrogenation of m-dinitrobenzene over alumina supported Au and Au–Ni alloy. Catal Lett. 2009;127:25–32.

9. Nutt MO, Heck KN, Alvarez P, Wong MS. Improved Pd-on-Au bimetallic nanoparticle catalysts for aqueous-phase trichloroethene hydrodechlorination. Appl Catal B. 2006;69:115–25.

10. Boccuzzi F, Chiorino A, Manzoli M, Lu P, Akita T, Ichikawa S, et al. Au/TiO$_2$ nanosized samples: a catalytic, TEM, and FTIR study of the effect of calcination temperature on the CO oxidation. J Catal. 2001;202:256–67.

11. Lopez N, Janssens TVW, Clausen BS, Xu Y, Mavrikakis M, Bligaard T, et al. On the origin of the catalytic activity of gold nanoparticles for low-temperature CO oxidation. J Catal. 2004;223:232–5.

12. Ivanova S, Pitchon V, Zimmermann Y, Petit C. Preparation of alumina supported gold catalysts: influence of washing procedures, mechanism of particles size growth. Appl Catal A. 2006;298:57–64.

13. Daté M, Okumura M, Tsubota S, Haruta M. Vital role of moisture in the catalytic activity of supported gold nanoparticles. Angew Chem Int Ed Engl. 2004;43:2129–32.

14. Schubert MM, Hackenberg S, van Veen AC, Muhler M, Plzak V, Behm RJ. CO Oxidation over supported gold catalysts—"inert" and "active" support materials and their role for the oxygen supply during reaction. J Catal. 2001;197:113–22.

15. Bond GC, Thompson DT. Gold-catalysed oxidation of carbon monoxide. Gold Bull. 2000;33:41–50.

16. Gluhoi AC, Bogdanchikova N, Nieuwenhuys BE. The effect of different types of additives on the catalytic activity of Au/Al$_2$O$_3$ in propene total oxidation: transition metal oxides and ceria. J Catal. 2005;229:154–62.

17. Wang L-C, Huang X-S, Liu Q, Liu Y-M, Cao Y, He H-Y, et al. Gold nanoparticles deposited on manganese(III) oxide as novel efficient catalyst for low temperature CO oxidation. J Catal. 2008;259:66–74.

18. Dekker MAP, Lippits MJ, Nieuwenhuys BE. Supported gold/MOx catalysts for NO/H$_2$ and CO/O$_2$ reactions. Catal Today. 1999;54:381–90.

19. Mariño F, Descorme C, Duprez D. Supported base metal catalysts for the preferential oxidation of carbon monoxide in the presence of excess hydrogen (PROX). Appl Catal B. 2005;58:175–83.

20. Centeno MA, Paulis M, Montes M, Odriozola JA. Catalytic combustion of volatile organic compounds on Au/CeO$_2$/Al$_2$O$_3$ and Au/Al$_2$O$_3$ catalysts. Appl Catal A. 2002;234:65–78.

21. Wang D, Haob Z, Chenga D, Shi X, Hub C. Influence of pretreatment conditions on low-temperature CO oxidation over Au/MOx/Al$_2$O$_3$ catalysts. J Mol Catal A. 2003;200:229–38.

22. Grisel RJH, Nieuwenhuys BE. A comparative study of the oxidation of CO and CH$_4$ over Au/MO$_x$/Al$_2$O$_3$ catalysts. Catal Today. 2001;64:69–81.

23. Gluhoi AC, Dekkers MAP, Nieuwenhuys BE. Comparative studies of the N$_2$O/H$_2$, N$_2$O/CO, H$_2$/O$_2$ and CO/O$_2$ reactions on supported gold catalysts: effect of the addition of various oxides. J Catal. 2003;219:197–205.

24. Grisel RJH, Westrate CJ, Goossens A, Craje MWJ, van der Kraan AM, Nieuwenhuys BE. Oxidation of CO over Au/MO$_x$/Al$_2$O$_3$ multi-component catalysts in a hydrogen-rich environment. Catal Today. 2002;72:123–32.

25. Bakrania SD, Rathore GK, Wooldridge MS. An investigation of the thermal decomposition of gold acetate. J Therm Anal Calorim. 2009;95:117–22.

26. Li WB, Wang JX, Gong H. Catalytic combustion of VOCs on non-noble metal catalysts. Catal Today. 2009;148:81–7.

27. Morales MR, Barbero BP, Cadůs LE. Evaluation and characterization of Mn–Cu mixed oxide catalysts for ethanol total oxidation: influence of copper content. Fuel. 2008;87:1177–86.

28. Wang L-C, He L, Liu Y-M, Cao Y, He H-Y, Fan K-N, et al. Effect of pretreatment atmosphere on CO oxidation over α-Mn$_2$O$_3$ supported gold catalysts. J Catal. 2009;264:145–53.

29. Wang L-C, Liu Q, Huang X-S, Liu Y-M, Cao Y, Fan K-N. Gold nanoparticles supported on manganese oxides for low-temperature CO oxidation. Appl Catal B. 2009;88:204–12.

30. Shaheen WM, Hong KS. Thermal characterization and physicochemical properties of Fe$_2$O$_3$–Mn$_2$O$_3$/Al$_2$O$_3$ system. Thermochim Acta. 2002;381:153–64.

31. Ramirez-Ortiz J, Ogura T, Medina-Valtierra J, Acosta-Ortiz SE, Bosh P, de los Reyes JA, et al. A catalytic application of Cu$_2$O and CuO films deposited over fiberglass. Appl Surf Sci. 2001;174(3–4):177–84.

32. Kim S-K, Kim K-H, Ihm S-K. The characteristics of wet air oxidation of phenol over CuO$_x$/Al$_2$O$_3$ catalysts: effect of copper loading. Chemosphere. 2007;68:287–92.

33. Mendes D, Garcia H, Silva VB, Mendes A, Madeira LM. Comparison of nanosized gold-based and cooper catalysts for the low-temperature water-gas shift reaction. Ind Eng Chem Res. 2009;48:430–9.

34. Saitzek S, Villain S, Nolibé G, Gavarri JR. Electrical behaviour of catalytic nanostructured CeO$_2$/CuO$_x$ composites under air–methane gas impulses. Appl Surf Sci. 2007;253:7490–6.

35. Liu J, Wang S, Wang Q, Geng B. Microwave chemical route to self-assembled quasi-spherical Cu$_2$O microarchitectures and their gas-sensing properties. Sens Actuators B. 2009;143:253–60.

36. Wang Ch-H, Lin S-S, Chen Ch-L, Weng H-S. Performance of the supported copper oxide catalysts for the catalytic incineration of aromatic hydrocarbons. Chemosphere. 2006;64:503–9.

37. Avgouropoulos G, Ioannides T. Effect of synthesis parameters on catalytic properties of CuO-CeO$_2$. Appl Catal B. 2006;67:1–11.

38. Mariño F, Baronetti G, Laborde M, Bion N, Le Valant A, Epron F, et al. Optimized CuO–CeO$_2$ catalysts for COPROX reaction. Int J Hydrogen Energy. 2008;33:1345–53.

39. Kucza W, Obłąkowski J, Gajerski R, Łabuś S, Danielewski M, Małecki A, et al. Synthesis and characterization of alumina- and zirconia-based powders obtained by the ultrasonic spray pyrolysis. J Therm Anal Calorim. 2007;88:65–9.

40. Delmon B. Preparation of heterogeneous catalysts. Synthesis of highly dispersed solids and their reactivity. J Therm Anal Calorim. 2007;90:49–65.

41. Małecki A, Gajerski R, Łabuś S, Prochowska-Klisch B, Wojciechowski KT. Mechanism of thermal decomposition of d-metals nitrates hydrates. J Therm Anal Calorim. 2000;60:17–23.

42. Tsuchida T, Sakata A, Furuichi R, Ishii T. Reactivity of amorphous aluminas prepared by the thermal decomposition of aluminum chloride and nitrate. Thermochim Acta. 1981;43:91–102.

43. Malecka B. Thermal decomposition of selected d-metal oxysalts. Kraków: Uczelniane Wydawnictwa Naukowo-Dydaktyczne AGH; 2005.